

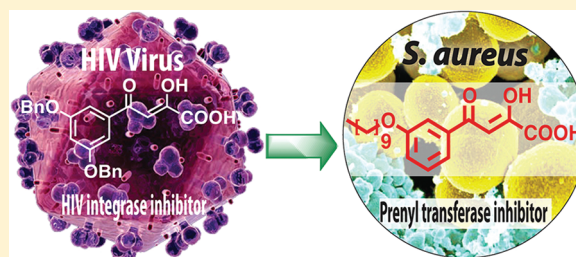
HIV-1 Integrase Inhibitor-Inspired Antibacterials Targeting Isoprenoid Biosynthesis

Yonghui Zhang,^{*,†,‡} Fu-Yang Lin,^{§,○} Kai Li,^{‡,○} Wei Zhu,[§] Yi-Liang Liu,[§] Rong Cao,[‡] Ran Pang,^{||} Eunhae Lee,^{||} Jordan Axelson,[‡] Mary Hensler,[∇] Ke Wang,[‡] Katie J. Molohon,[⊥] Yang Wang,[‡] Douglas A. Mitchell,^{‡,⊥,#} Victor Nizet,[∇] and Eric Oldfield^{*,‡,§}[†]PrenylX Research Institute, Zhangjiagang, 215600, People's Republic of China[‡]Department of Chemistry, [§]Center for Biophysics & Computational Biology, ^{||}School of Molecular and Cellular Biology,[⊥]Department of Microbiology, and [#]Institute for Genomic Biology, University of Illinois at Urbana–Champaign, Urbana, Illinois 61801, United States[∇]Department of Pediatrics and Skaggs School of Pharmacy and Pharmaceutical Sciences, University of California, San Diego, La Jolla, California 92093, United States

S Supporting Information

ABSTRACT: We report the discovery of antibacterial leads, keto- and diketo-acids, targeting two prenyl transferases: undecaprenyl diphosphate synthase (UPPS) and dehydrosqualene synthase (CrtM). The leads were suggested by the observation that keto- and diketo-acids bind to the active site Mg²⁺/Asp domain in HIV-1 integrase, and similar domains are present in prenyl transferases. We report the X-ray crystallographic structures of one diketo-acid and one keto-acid bound to CrtM, which supports the Mg²⁺ binding hypothesis, together with the X-ray structure of one diketo-acid bound to UPPS. In all cases, the inhibitors bind to a farnesyl diphosphate substrate-binding site. Compound 45 had cell growth inhibition MIC₉₀ values of ~250–500 ng/mL against *Staphylococcus aureus*, 500 ng/mL against *Bacillus anthracis*, 4 μg/mL against *Listeria monocytogenes* and *Enterococcus faecium*, and 1 μg/mL against *Streptococcus pyogenes* M1 but very little activity against *Escherichia coli* (DH5α, K12) or human cell lines.

KEYWORDS: antibacterials, isoprenoid biosynthesis, HIV integrase, undecaprenyl diphosphate synthase, dehydrosqualene synthase



There is currently an urgent need for new types of antibacterials exhibiting novel modes of action, due to the rapid rise in drug resistance,¹ and isoprenoid biosynthesis^{2,3} is one attractive target. For example, cell wall biosynthesis can be inhibited by targeting farnesyl diphosphate synthase (FPPS) or undecaprenyl diphosphate synthase (UPPS), involved in lipid I biosynthesis (Figure 1). In addition, in *Staphylococcus aureus*, the formation of the virulence factor staphyloxanthin⁴ can be blocked by inhibiting dehydrosqualene synthase (CrtM), resulting in a lowering of the antioxidant shield to host derived reactive oxygen species (ROS)⁵ (Figure 1). The bisphosphonate class of drugs such as zoledronate (**1**, Chart 1) are potent, low nanomolar inhibitors of FPPS, but **1** has little antibacterial activity (presumably due to lack of cell penetration), although more lipophilic bisphosphonates such as **2** (BPH-210, Chart 1) have modest activity (IC₅₀ ~ 30 μM) against *Escherichia coli*.⁶ More lipophilic bisphosphonates also potentially target UPPS,⁷ as well as CrtM,⁵ but again, they have essentially no activity in bacteria. Replacing one phosphonate group by a sulfonate to form a phosphonosulfonate results, however, in potent CrtM inhibitors (e.g., **3**, BPH-652, Chart 1, IC₅₀ ~ 7.9 μM, K_i ~ 80 nM) that also blocks carotenoid pigment formation in cells (IC₅₀ ~ 110 nM).⁸ In addition, there has recently been interest

in developing phosphorus-free prenyl transferase inhibitors, which might have even more druglike properties. For example, Jahnke et al. reported a series of FPPS inhibitors, dicarboxylic acids, that bound to a novel, allosteric site.⁹ In addition, other species such as tetramic acid UPPS inhibitors have been described (e.g., **4**, Chart 1),¹⁰ but to date, their X-ray structures have not been reported, although an allosteric model has been proposed.¹¹

A key component of the active site of most prenyl transferases is a Mg²⁺/Asp motif that interacts with a substrate's diphosphate group. We reasoned that HIV-1 integrase (IN) inhibitors¹² might provide clues for new prenyl transferase inhibitors, since IN contains a similar Asp/Mg²⁺ motif¹³ and IN inhibitors such as **5** (L-708,906, Chart 1)¹⁴ and **6** (elvitegravir, Chart 1),¹⁵ diketo-acids and keto-acids, respectively, are thought to bind at or near the Mg²⁺/Asp motif in the IN active site.^{16,17} In addition, many other IN inhibitors like raltegravir, dolutegravir, MK2048, etc. (structures not shown) have been found to bind Mg²⁺.^{17–19}

Received: February 12, 2012

Accepted: April 3, 2012

Published: April 3, 2012

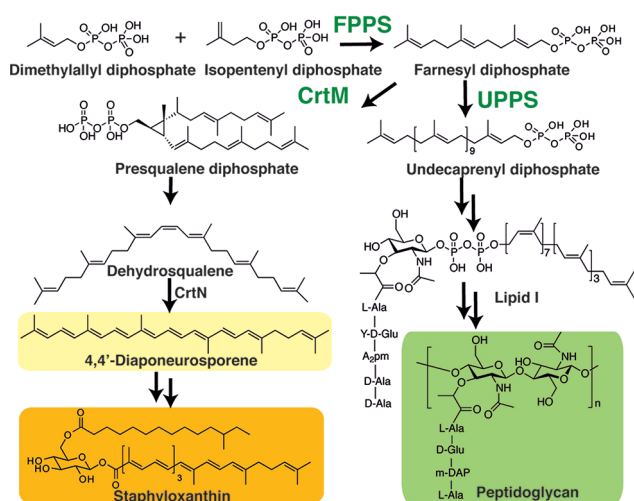


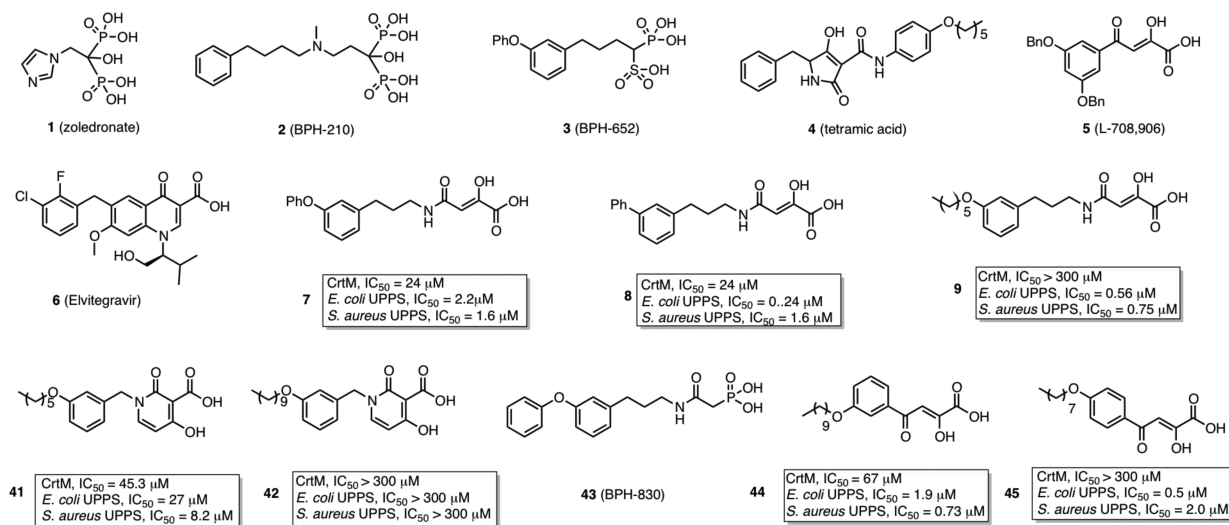
Figure 1. Biosynthetic reactions catalyzed by CrtM and UPPS, with the end products of the pathways shown.

We thus made a small screening library (38 compounds) of IN inhibitor-inspired molecules and their structures, and inhibition of *S. aureus* CrtM, *E. coli* UPPS, and *S. aureus* UPPS are shown in Figure S1 in the Supporting Information. Most compounds were amide-diketo acids (7–40, class I, Figure S1 in the Supporting Information) and were conveniently prepared from the synthon (*Z*)-2,2-dimethyl-5-carboxymethylene-1,3-dioxolan-4-one²⁰ by amine coupling. Among these compounds, 7 (Chart 1) inhibited CrtM with $IC_{50} \sim 24 \mu\text{M}$, $K_i \sim 250 \text{ nM}$ (for comparison, K_i of 3 $\sim 70 \text{ nM}$ ⁸) and blocked staphyloxanthin pigment formation ($IC_{50} = 4 \mu\text{M}$). Inhibitors of class II were keto-acids, dihydropyridone-3-carboxylates, and were based on 6 (Elvitegravir) and dihydroquinoline-3-carboxylic acid IN inhibitors,²¹ which again are thought to bind via their carboxyl and carbonyl oxygens to Mg^{2+}/Asp .²² We made two analogues, 41 and 42 (Chart 1), with alkoxy-aryl tails to mimic the substrate farnesyl diphosphate (FPP). The longer chain species 42 had no activity, but the shorter chain species 41 had a CrtM $IC_{50} = 45 \mu\text{M}$, $K_i = 450 \text{ nM}$, and a loss of pigmentation $IC_{50} = 33 \mu\text{M}$.

To see how these inhibitors bound to CrtM, we carried out cocrystallization and soaking experiments with 7 (class I) and 41 (class II) and obtained crystals (by soaking) that diffracted to 2.3 and 1.9 Å, respectively. Full X-ray crystallographic data and structure refinement details are given in the Supporting Information, Table S1. Electron density results for 7 are shown in Figure 2a and indicate the presence of 7 in addition to one molecule of farnesyl monophosphate (FMP) that copurified with the protein. The identity of FMP was further confirmed by LC-MS (Supporting Information, Figure S2) and the electron density results (Figure 2a). The diphenyl ether fragment in 7 (cyan) binds into the CrtM S1 site²³ and is shown in Figure 2b superimposed on one of the *S*-thio-farnesyl diphosphate (FSPP) inhibitors (in yellow, green) whose structures were reported previously.⁵ This binding mode is similar to that seen with the phosphonosulfonate 3 (Figure 2c), with the diketo-acid headgroup interacting with two of the three Mg^{2+} ($Mg^{2+}_{B,C}$) seen in the CrtM-FSPP structure (Figure 2d). The farnesyl side chain in FMP bound to the S2 site and had a 0.8 Å rmsd from the S2 FSPP reported previously.⁵ With 41, the ligand electron density is again well-defined (Figure 3a), and the crystallographic results show that the side chain binds in S2, similar to the farnesyl side chain in the FSPP structures (Figure 3b), as well as the phosphonoacetamide analogue of 7 (43, BPH-830,²⁴ Figure 3c). There are three Mg^{2+} in the X-ray structure. However, these are not the Mg^{2+}_{ABC} seen in most prenyl transferases²⁵ but rather Mg^{2+}_{BCD} . That is, there is a new Mg^{2+} binding site, Mg^{2+}_D . The dihydropyridone side chain interacts with Mg^{2+}_{CD} but, surprisingly, via the two ring oxygens, not the carboxylate (Figure 3d), which interacts with two water molecules (Supporting Information, Figure S3). These inhibition and structural results for 7 and 41 clearly support the Mg^{2+} binding hypothesis, at least for CrtM.

CrtM is a so-called head-to-head prenyl transferase so we next sought to see if any of the molecules synthesized might also inhibit the head-to-tail prenyl transferase FPPS or the *cis*-prenyl transferase, UPPS. There was no activity against FPPS (probably due to the lack of a positively charged feature that mimics the carbocation involved in FPP biosynthesis), but most of the amide-diketo acids (class I) were potent UPPS inhibitors

Chart 1. Chemical Structures of Selected Compounds and the Inhibition of CrtM, *E. coli* UPPS, and *S. aureus* UPPS by 7–9, 41, 42, 44, and 45



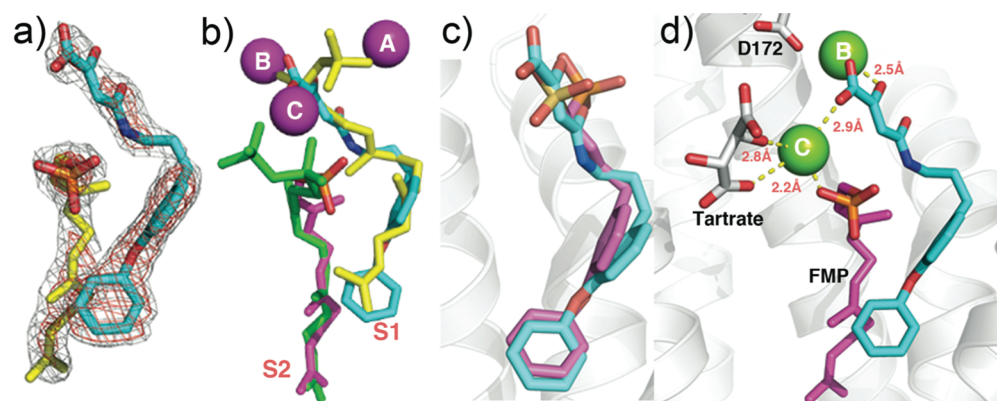


Figure 2. CrtM crystallographic structures. (a) Compound 7 (cyan) plus FMP (yellow) electron density, bound to CrtM. (b) Compound 7 (cyan) bound to CrtM, superimposed on two FSPP molecules (yellow, green; PDB ID code 2ZCP). Also shown is the FMP (magenta) that cocrystallized. The Mg^{2+} are from the FSPP structure. (c) Comparison between 7 (cyan) and 3 (magenta, PDB ID code 2ZCQ) bound to CrtM. Both diphenyl ether side chains bind in S1. (d) Interactions between 7 (cyan), FMP (magenta), and Mg^{2+} in CrtM.

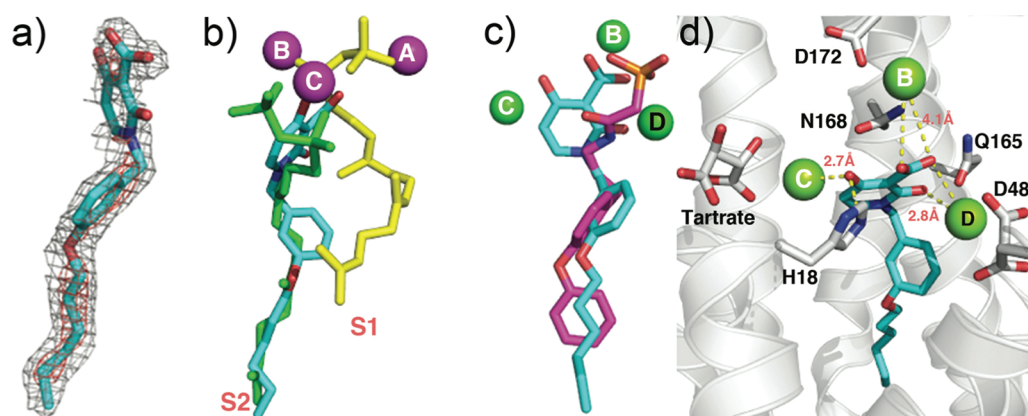


Figure 3. CrtM crystallographic structures. (a) Electron density of 41 bound to CrtM. (b) Structure of 41 (cyan) bound to CrtM shown superimposed on two FSPP molecules (yellow, green). (c) Comparison between 41 (cyan) and the phosphonoacetamide analog of 7 (compound 43, BPH-830)²⁴ (magenta) bound to CrtM (PDB ID code 2ZY1). (d) Interactions between 41 (cyan) and Mg^{2+} in CrtM.

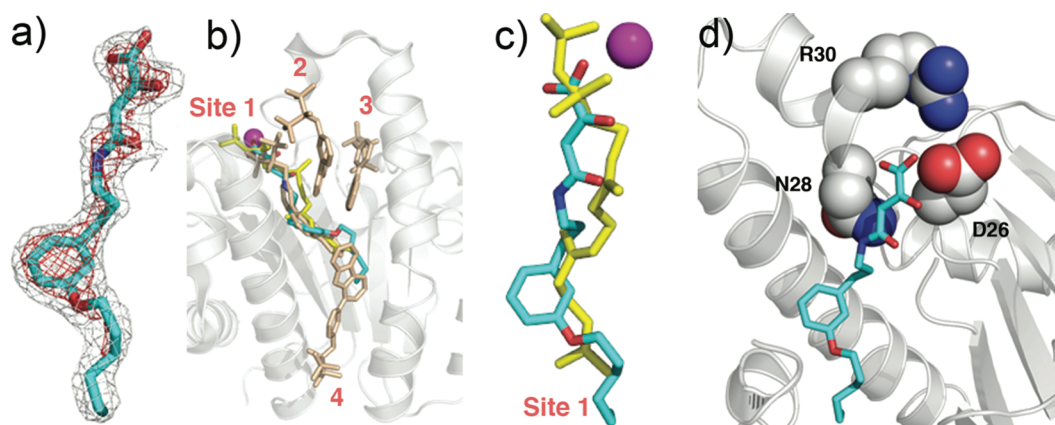


Figure 4. UPPS crystallographic structures. (a) Electron density of 9 bound to UPPS. (b) Structure of 9 (cyan) bound to UPPS, superimposed on FSPP/ Mg^{2+} (from PDB ID code 1X06) and four bisphosphonate inhibitors (PDB ID code 2E98). (c) Superposition of 9 (cyan) on FSPP (yellow) in site 1 in UPPS. The Mg^{2+} is from the FSPP structure. (d) The diketo-acid headgroup of 9 binds into the active site of UPPS and interacts with D26 and N28.

with the most active one (8) having an $IC_{50} \sim 240$ nM and $K_i \sim 120$ nM, comparable to the most active bisphosphonate UPPS inhibitor BPH-629 ($IC_{50} \sim 300$ nM for *E. coli* UPPS).⁷ There are four different ligand-binding sites in UPPS (designated 1–4 in ref 7) found with bisphosphonate inhibitors. This is not unexpected since the UPPS product,

undecaprenyl diphosphate (UPP), contains 55-carbon atoms and is thus much larger than the (C_{15}) FPP substrate. In principle, then, novel inhibitors might occupy multiple binding sites.

Cocrystallization of *E. coli* UPPS with 9 ($IC_{50} = 560$ nM) produced well-formed crystals with *E. coli* UPPS, and the

electron density was well resolved (Figure 4a). As can be seen in Figure 4b, **9** binds to site 1,⁷ the FPP binding site, and as can be seen in Figure 4c, **9** (in cyan) closely maps the FPP backbone structure (in yellow) with the diketo-acid fragment being located close to two of the three essential residues in UPPS, D26 and N28 (Figure 4d). We found no evidence for the presence of Mg²⁺, but this observation is not entirely unexpected since even with the five *E. coli* UPPS X-ray structures with strong Mg²⁺ chelators, bisphosphonates (PDB ID codes 2E98, 2E99, 2E9A, 2E9C, and 2E9D),⁷ Mg²⁺ was not observed.

The amide-diketo acids were not growth suppressive toward *S. aureus* or *E. coli*, perhaps due to the instability of the amide bond inside the cells or a lack of cell permeability. However, **44** and **45** (aryldiketo acids, class III) had good activity against *S. aureus* UPPS (**44**, IC₅₀ = 0.73 μM, K_i = 230 nM; **45**, IC₅₀ = 2.0 μM, K_i = 670 nM), and both were active against the USA300 (MRSA) strain of *S. aureus* with MIC₉₀ values of 500 (**44**) and 250–500 ng/mL (**45**). There was no appreciable activity against the Gram-negative *E. coli*; however, there was promising activity against other Gram-positives: ~ 500 ng/mL against *Bacillus anthracis* str. Sterne, ~ 4 μg/mL against *Listeria monocytogenes* and *Enterococcus faecium* U503, and ~1 μg/mL for *Streptococcus pyogenes* M1. While the precise mechanism of action of these compounds in each cell remains to be determined, UPPS inhibition is a likely candidate. In addition, we found low toxicity against a human cell line (MCF-7; IC₅₀ ~ 30 μM), consistent with poor FPPS inhibition.

These results are important for several reasons. First, we tested the hypothesis that keto- and diketo-acids might inhibit prenyl transferase enzymes, based on the presence of Mg²⁺/Asp motifs in their active sites—an “integrase inhibitor-inspired” approach. The best CrtM inhibitors had K_i ~ 250 nM and were active in blocking staphyloxanthin biosynthesis in *S. aureus*, and we solved two structures of lead compounds bound to CrtM. In both, the inhibitor head groups bound to Mg²⁺, while the side chains bound to one or the other of the two FPP side chain binding sites. Second, we tested this small library for FPPS and UPPS inhibition. There was no FPPS inhibition, but the most potent UPPS inhibitor had an IC₅₀ = 240 nM, and we determined the structure of one such lead bound to *E. coli* UPPS—the first UPPS X-ray structure reported for a nonbisphosphonate inhibitor. We also found low toxicity and promising activity against a subset of Gram-positive bacteria with MIC₉₀ values as low as 250–500 ng/mL against USA300 *S. aureus* and 500 ng/mL against *Bacillus anthracis* str. Sterne and low activity against *E. coli* and a human cell line. Overall, these results indicate that integrase-inspired inhibitors may be engineered into drug leads that target isoprenoid biosynthesis.

■ ASSOCIATED CONTENT

Supporting Information

X-ray study, synthesis, and characterization of the screening library compounds. This material is available free of charge via the Internet at <http://pubs.acs.org>.

■ AUTHOR INFORMATION

Corresponding Author

*E-mail: yhzhang30@yahoo.com (Y.Z.) or eo@chad.scs.uiuc.edu (E.O.).

Author Contributions

[○]These authors contributed equally.

Funding

This work was supported by the U.S. Public Health Service (NIH Grant SR01AI074233-16 to E.O.) and the NIH Director's New Innovator Award Program (DP2 OD008463 to D.A.M.). K.J.M. was supported in part by a NIH Cellular and Molecular Biology Training Grant (T32 GM007283). The Advanced Photon Source was supported by Department of Energy Contract DE-AC02-06CH11357. The Life Science Collaborative Access Team Sector 21 was supported by the Michigan Economic Development Corporation and Michigan Technology Tri-Corridor (Grant 085P000817).

Notes

The authors declare no competing financial interest.

■ ACKNOWLEDGMENTS

We thank Andrew H.-J. Wang of the Institute of Biological Chemistry, Academia Sinica (Taipei, Taiwan), for providing *E. coli* UPPS plasmids and *S. aureus* CrtM plasmids.

■ ABBREVIATIONS

CrtM, dehydrosqualene synthase; UPPS, undecaprenyl diphosphate synthase; FPPS, farnesyl diphosphate synthase; FPP, farnesyl diphosphate; FMP, farnesyl monophosphate; FSPP, S-thiolo-farnesyl diphosphate; IN, HIV-1 integrase

■ REFERENCES

- (1) Walsh, C. T.; Fischbach, M. A. Repurposing libraries of eukaryotic protein kinase inhibitors for antibiotic discovery. *Proc. Natl. Acad. Sci. U.S.A.* **2009**, *106*, 1689–1690.
- (2) Oldfield, E. Targeting isoprenoid biosynthesis for drug discovery: Bench to bedside. *Acc. Chem. Res.* **2010**, *43*, 1216–1226.
- (3) Oldfield, E.; Lin, F. Y. Terpene biosynthesis: Modularity rules. *Angew. Chem., Int. Ed. Engl.* **2012**, *51*, 1124–1137.
- (4) Liu, G. Y.; Essex, A.; Buchanan, J. T.; Datta, V.; Hoffman, H. M.; Bastian, J. F.; Fierer, J.; Nizet, V. *Staphylococcus aureus* golden pigment impairs neutrophil killing and promotes virulence through its antioxidant activity. *J. Exp. Med.* **2005**, *202*, 209–215.
- (5) Liu, C. I.; Liu, G. Y.; Song, Y.; Yin, F.; Hensler, M. E.; Jeng, W. Y.; Nizet, V.; Wang, A. H.; Oldfield, E. A cholesterol biosynthesis inhibitor blocks *Staphylococcus aureus* virulence. *Science* **2008**, *319*, 1391–1394.
- (6) Leon, A.; Liu, L.; Yang, Y.; Hudock, M. P.; Hall, P.; Yin, F.; Studer, D.; Puan, K. J.; Morita, C. T.; Oldfield, E. Isoprenoid biosynthesis as a drug target: Bisphosphonate inhibition of *Escherichia coli* K12 growth and synergistic effects of fosmidomycin. *J. Med. Chem.* **2006**, *49*, 7331–7341.
- (7) Guo, R. T.; Cao, R.; Liang, P. H.; Ko, T. P.; Chang, T. H.; Hudock, M. P.; Jeng, W. Y.; Chen, C. K.; Zhang, Y.; Song, Y.; Kuo, C. J.; Yin, F.; Oldfield, E.; Wang, A. H. Bisphosphonates target multiple sites in both *cis*- and *trans*-prenyltransferases. *Proc. Natl. Acad. Sci. U.S.A.* **2007**, *104*, 10022–10027.
- (8) Song, Y.; Lin, F. Y.; Yin, F.; Hensler, M.; Rodrigues Poveda, C. A.; Mukkamala, D.; Cao, R.; Wang, H.; Morita, C. T.; Gonzalez Pacanowska, D.; Nizet, V.; Oldfield, E. Phosphonosulfonates are potent, selective inhibitors of dehydrosqualene synthase and staphyloxanthin biosynthesis in *Staphylococcus aureus*. *J. Med. Chem.* **2009**, *52*, 976–988.
- (9) Jahnke, W.; Rondeau, J. M.; Cotesta, S.; Marzinzik, A.; Pelle, X.; Geiser, M.; Strauss, A.; Gotte, M.; Bitsch, F.; Hemmig, R.; Henry, C.; Lehmann, S.; Glickman, J. F.; Roddy, T. P.; Stout, S. J.; Green, J. R. Allosteric non-bisphosphonate FPPS inhibitors identified by fragment-based discovery. *Nat. Chem. Biol.* **2010**, *6*, 660–666.
- (10) Peukert, S.; Sun, Y.; Zhang, R.; Hurley, B.; Sabio, M.; Shen, X.; Gray, C.; Dzink-Fox, J.; Tao, J.; Cebula, R.; Wattanasin, S. Design and structure-activity relationships of potent and selective inhibitors of undecaprenyl pyrophosphate synthase (UPPS): Tetramic, tetriconic

acids and dihydropyridin-2-ones. *Bioorg. Med. Chem. Lett.* **2008**, *18*, 1840–1884.

(11) Lee, L. V.; Granda, B.; Dean, K.; Tao, J.; Liu, E.; Zhang, R.; Peukert, S.; Wattanasin, S.; Xie, X.; Ryder, N. S.; Tommasi, R.; Deng, G. Biophysical investigation of the mode of inhibition of tetramic acids, the allosteric inhibitors of undecaprenyl pyrophosphate synthase. *Biochemistry* **2010**, *49*, 5366–5376.

(12) For a review, see Neamati, N. *HIV-1 Integrase: Mechanism and Inhibitor Design*; John Wiley & Sons Inc.: Hoboken, NJ, 2011.

(13) Goldgur, Y.; Dyda, F.; Hickman, A. B.; Jenkins, T. M.; Craigie, R.; Davies, D. R. Three new structures of the core domain of HIV-1 integrase: an active site that binds magnesium. *Proc. Natl. Acad. Sci. U.S.A.* **1998**, *95*, 9150–9154.

(14) Hazuda, D. J.; Felock, P.; Witmer, M.; Wolfe, A.; Stillmock, K.; Grobler, J. A.; Espeseth, A.; Gabryelski, L.; Schleif, W.; Blau, C.; Miller, M. D. Inhibitors of strand transfer that prevent integration and inhibit HIV-1 replication in cells. *Science* **2000**, *287*, 646–650.

(15) Sato, M.; Kawakami, H.; Motomura, T.; Aramaki, H.; Matsuda, T.; Yamashita, M.; Ito, Y.; Matsuzaki, Y.; Yamataka, K.; Ikeda, S.; Shinkai, H. Quinolone carboxylic acids as a novel monoketo acid class of human immunodeficiency virus type 1 integrase inhibitors. *J. Med. Chem.* **2009**, *52*, 4869–4882.

(16) Grobler, J. A.; Stillmock, K.; Hu, B.; Witmer, M.; Felock, P.; Espeseth, A. S.; Wolfe, A.; Egbertson, M.; Bourgeois, M.; Melamed, J.; Wai, J. S.; Young, S.; Vacca, J.; Hazuda, D. J. Diketo acid inhibitor mechanism and HIV-1 integrase: Implications for metal binding in the active site of phosphotransferase enzymes. *Proc. Natl. Acad. Sci. U.S.A.* **2002**, *99*, 6661–6666.

(17) Hare, S.; Gupta, S. S.; Valkov, E.; Engelman, A.; Cherepanov, P. Retroviral intasome assembly and inhibition of DNA strand transfer. *Nature* **2010**, *464*, 232–236.

(18) Hare, S.; Smith, S. J.; Métifiot, M.; Jaxa-Chamiec, A.; Pommier, Y.; Hughes, S.; Cherepanov, P. Structural and functional analyses of the second-generation integrase strand transfer inhibitor dolutegravir (S/GSK 1349572). *Mol. Pharmacol.* **2011**, *80*, 565–572.

(19) Hare, S.; Vos, A. M.; Clayton, R. F.; Thuring, J. W.; Cummings, M. D.; Cherepanov, P. Molecular mechanisms of retroviral integrase inhibition and the evolution of viral resistance. *Proc. Natl. Acad. Sci. U.S.A.* **2010**, *107*, 20057–20062.

(20) Zhu, K.; Simpson, J. H.; Delaney, E. J.; Nugent, W. A. Synthesis of Z-5-carboxymethylene-1,3-dioxolan-4-ones: A better way. *J. Org. Chem.* **2007**, *72*, 3949–3951.

(21) Sechi, M.; Rizzi, G.; Bacchi, A.; Carcelli, M.; Rogolino, D.; Pala, N.; Sanchez, T. W.; Taheri, L.; Dayam, R.; Neamati, N. Design and synthesis of novel dihydroquinoline-3-carboxylic acids as HIV-1 integrase inhibitors. *Bioorg. Med. Chem.* **2009**, *17*, 2925–2935.

(22) Vandurm, P.; Cauvin, C.; Guiguen, A.; Georges, B.; Le Van, K.; Martinelli, V.; Cardona, C.; Mbemba, G.; Mouscadet, J. F.; Hevesi, L.; Van Lint, C.; Wouters, J. Structural and theoretical studies of [6-bromo-1-(4-fluorophenylmethyl)-4(1H)-quinolinon-3-yl]-4-hydroxy-2-oxo-3-butenic acid as HIV-1 integrase inhibitor. *Bioorg. Med. Chem. Lett.* **2009**, *19*, 4806–4809.

(23) Lin, F. Y.; Liu, C. I.; Liu, Y. L.; Zhang, Y.; Wang, K.; Jeng, W. Y.; Ko, T. P.; Cao, R.; Wang, A. H.; Oldfield, E. Mechanism of action and inhibition of dehydrosqualene synthase. *Proc. Natl. Acad. Sci. U.S.A.* **2010**, *107*, 21337–21342.

(24) Song, Y.; Liu, C. I.; Lin, F. Y.; No, J. H.; Hensler, M.; Liu, Y. L.; Jeng, W. Y.; Low, J.; Liu, G. Y.; Nizet, V.; Wang, A. H.; Oldfield, E. Inhibition of staphyloxanthin virulence factor biosynthesis in *Staphylococcus aureus*: In vitro, in vivo, and crystallographic results. *J. Med. Chem.* **2009**, *52*, 3869–3880.

(25) Aaron, J. A.; Christianson, D. W. Trinuclear Metal Clusters in Catalysis by Terpenoid Synthases. *Pure Appl. Chem.* **2010**, *82*, 1585–1597.